Technical Report

Quantitative Analysis of the Size Distribution and the Number Concentration of NbC Fine Particles in Steels Using Asymmetric Flow Field-flow Fractionation (AF4)–ICP-MS Method

Daisuke ITABASHI* Shunsuke TANIGUCHI
Kazumi MIZUKAMI

Abstract

Application of asymmetric flow field-flow fractionation (AF4) with inductively coupled plasma–mass spectrometry (ICP–MS) for the analysis of fine precipitates in steels was investigated using various nano particles and niobium carbide (NbC) precipitates in steels. The performance of the size measurement by the AF4 results was investigated by comparing the measurement results of gold nanoparticles between AF4 and transmission electron microscopy (TEM). In addition, the broadening factors were devised to correct the particle size distribution measured by AF4. The quantification method of number concentration using the flow injection method (FI) was investigated and the accuracy of the quantification results was evaluated based on the recovery rate. The newly developed FI-AF4-ICP-MS method was applied for analysis of NbC in ferrite steels, and its performance was verified.

1. Introduction

In the development of steel materials, fine particles with particle sizes ranging from nanometers to submicrometers are utilized to give various mechanical properties to products.[1, 2] Nanometer-sized precipitates play a crucial role in precipitation strengthening[1] and grain size control[3] of steel. Since the size distribution and number concentration of precipitates influence the mechanical properties of steel, they must be accurately evaluated to determine alloy design and process conditions in steel manufacturing. In many steels, precipitates often exhibit a broad particle size distribution (e.g., a mixture of particles ranging from several nanometers to several hundred nanometers) and exist in a non-uniformly dispersed state. This makes it difficult to apply electron microscopy, which is limited to localized observation areas. Furthermore, while conventional chemical analysis methods for precipitates and inclusions have been applied to various steel samples, these methods dissolve precipitates and inclusions using acids[4] or alkalis, making it impossible to obtain size information.

To accurately measure the particle size distribution of mixtures containing particles with different sizes, it is necessary to separate the particles by size using some method before measuring the particle size of the sample. Many separation analysis methods based on particle size differences have been reported in previous studies, such as size exclusion chromatography,[5, 6] asymmetric flow field-flow fractionation (AF4),[7] hydrodynamic chromatography,[7] capillary electrophoresis,[8] gel electrophoresis,[9] and ultracentrifugation. Among these, AF4 has been reported in many reports as having several advantages for analyzing metal nanoparticles.[10, 11] It has been applied to various samples ranging from nanometers to micrometers, regardless of the presence of matrix components such as solvents, surfactants, or salts coexisting in the system.

The AF4 method does not require a stationary phase used in liquid chromatography separation columns and possesses the characteristic of achieving size-dependent separation. Furthermore, the AF4 method can be combined with various analytical methods such as light scattering analysis, ultraviolet-visible spectroscopy, induc-

* Ph.D., Senior Researcher, Materials Characterization Research Lab., Advanced Technology Research Laboratories
20-1 Shintomi, Futtsu City, Chiba Pref. 293-8511

tively coupled plasma–mass spectrometry (ICP–MS), and others as detection techniques. Especially, the combination with ICP-MS enables the acquisition of particle size distributions and elemental compositions of the separated samples. Therefore, AF4 is expected to be a useful technique for accurately measuring the particle size distribution of particles which is ununiformly distributed, with a broad size distribution (e.g., precipitates and inclusions in steels).

Therefore, in this study,[12, 13] we investigated methods for applying AF4 to evaluate steel samples. First, the performance of AF4 for particle size distribution measurement was investigated using gold nanoparticles (AuNPs). The accuracy of AF4 analysis was verified by comparing the measured results of the average particle size and distribution width of AuNPs obtained from AF4 and TEM. Furthermore, based on these results, a broadening factor was devised to correct the particle size distribution measured by AF4. Next, a quantitative method for AF4-ICP-MS analysis was developed (hereafter referred to as the FI-AF4-ICP-MS method). Flow injection (FI) chromatograms of metal element standard solutions, measured while mixed with the AF4 carrier solution, were integrated to create calibration curves. Furthermore, the accuracy of the quantitative values obtained by this method was evaluated based on the recovery rates of several types of gold nanoparticle (AuNP) standards. The developed FI-AF4-ICP-MS method was also applied to the analysis of niobium carbide (NbC) in ferritic steel to verify its applicability.

2. Experiments

2.1 Nanoparticles and reagents

In the experiment, it was utilized gold nanoparticles (AuNPs, nanoComposix (USA)), silver nanoparticles (AgNPs, nanoComposix (USA)), and size-standard polystyrene latex particles STADEX (PSL, JSR Life Science Corporation (Japan)). **Table 1** summarizes the specifications of the reference nanoparticles in water and tested specimens. Calibration curves for particle size measurement using AF4 were created with four types of AuNPs (AuNP-2, AuNP-5, AuNP-7, AuNP-10). AuNP-5.5 was prepared for comparison between AF4 and TEM. For AF4 measurements, AuNP-5.5 was measured in a water dispersion state. For TEM, a dispersion of AuNP-5.5 was also applied to a grid with a carbon-supporting grid, dried, and then observed using bright field (BF) imaging. Two types of AgNPs (sphere-like and plate-like, called AgNP-50s and AgNP-50p, respectively) were used for particle size distribution measurements by AF4 and TEM. Furthermore, for AF4 particle size measurements of each AgNP, the size calibration curve created using the AuNPs and PSL was employed. Five types of AuNPs (AuNP-5, AuNP-10, AuNP-30, AuNP-50, AuNP-100) were used to investigate recovery rates by the FI-AF4-ICP-MS method. Three types of AuNPs (AuNP-2, AuNP-5, AuNP-10) were used to calibrate the size measurements for the AF4 analysis of each steel specimens.

All reagents used for AF4-ICP-MS analysis were commercially available and used without additional purification. Dilution of sample solutions and preparation of AF4 carrier solutions were performed using ultrapure water (>18 MΩ: Milli-Q water purification system and Elix UV10, Millipore Corp. (USA)). Sodium dodecyl sulfate (SDS, purity≥99.0%, FUJIFILM Wako Pure Chemical Corporation (Japan)) and sodium cholate (SC, purity≥98.5%, FUJIFILM Wako Pure Chemical (Japan)) were used for preparing the AF4 carrier solution. For standard solution preparation, nitric acid (purity≥60.0–61.0%), hydrochloric acid (purity≥35.0–37.0%), and gold standard solution (Au1000, 1 000 mg L^{-1}, for atomic absorption spectrometry) from Kanto Chemical Co., Inc. (Japan) were used.

Table 1 Specifications of nanoparticles (specimen treated at 873 K for 1 h denoted as NCA5-1, at 873 K for 10 h denoted as NCA5-3)

Sample	Average diameter (nm)	Concentration (mg/L)	Dispersant	Shape
AuNP-2	2.1 ± 0.3	52.5	Glutathione	Sphere-like
AuNP-5	5.0 ± 0.6	1 080	Citrate	Sphere-like
AuNP-7	7.5 ± 0.8	1 070	Citrate	Sphere-like
AuNP-10	9.8 ± 0.8	1 080	Citrate	Sphere-like
PSL-29	29 ± 1	5 000	–	Sphere
PSL-48	48 ± 1	10 000	–	Sphere
PSL-70	70 ± 1	10 000	–	Sphere
PSL-100	100 ± 3	10 000	–	Sphere
AuNP-5.5	5.5 ± 0.5	1 090	Lipoic acid	Sphere-like
AgNP-50s	50 ± 4	20	Tannic acid	Sphere-like
AgNP-50p	55 ± 10	20	PVA	Plate-like
NbC precipitates in NCA5-1	–	–	SDS	Plate-like
NbC precipitates in NCA5-3	2.4 ± 1.0 (FOV-1) 2.1 ± 0.4 (FOV-2)	–	SDS	Plate-like

FOV: Field of view, PVA: Polyvinyl alcohol

For quantitative analysis of NbC in steel specimens by FI-AF4-ICP-MS, a multi-element standard solution (XSTC-8, 10 mg L^{-1}, SPEX CertiPrep (USA)) was used. Acetyl acetone (AA, special-grade, FUJIFILM Wako Pure Chemical), tetramethylammonium chloride (TMAC, purity≥98.0%, Tokyo Chemical Industry Co., Ltd.), and methanol (special-grade, FUJIFILM Wako Pure Chemical) were used to extract the NbC precipitates from the steel specimens.

2.2 Extraction of precipitates from steels and sample preparation by electrolytic dissolution

NbC-precipitated ferritic steel with a main chemical composition of 0.1Nb-0.01C (wt%) was prepared from electrolytic iron using vacuum induction melting. Block specimens (30 × 33 × 45 mm^3) for heat treatment were taken from an as-cast ingot. After solid solution treatment (1 523 K, 24 h) followed by water quenching, NbC was precipitated by holding at 873 K for 1 h (NCA5-1) or 10 h (NCA5-3). The particle size and number concentration of NbC were changed by adjusting the holding time at 873 K during the heat treatment. Additionally, the small specimens were cut into dimensions of 25 × 25 × 2 mm^3 for the following analysis.

To extract precipitates from steel specimens, the selective potentio-static etching by electrolytic dissolution (SPEED) method[14, 15] was applied. The electrolyte used was a 10% AA-based solution (10% (v/v) AA-1% (w/v) TMAC-methanol) to which SDS was added at a concentration of 500 μg mL^{-1} as a dispersant (hereinafter referred to as the SPEED solution). Here, adding SDS as a surfactant adsorbed onto the surface of the extracted precipitates prevents these precipitates from aggregating in the SPEED solution. The electrolytic extraction conditions were the same as previously reported, using constant-current electrolysis at 500 mA, and were conducted in the following two-step process. In the first step, a 15-minute electrolytic extraction was performed to dissolve the pollutants

and oxide layers on the surface of the steel sample. After completing the first step, the steel specimen was transferred to another SPEED solution with same composition. This operation separated and removed pollutants and oxide layers dissolved in the SPEED solution from the steel sample surface. The subsequent second step involved a 120-minute electrolytic extraction. This operation enabled the dissolution of approximately 1.0 g of steel anode sample into the SPEED solution. Subsequently, ultrasonic treatment was performed for 1 minute to disperse and collect all precipitates into the SPEED solution. AF4-ICP-MS analysis was performed on the solution sample containing these dispersed precipitates.

2.3 TEM observation

The AuNPs dispersed in solutions were placed on the carbon-supporting grid, dried under reduced pressure, and subjected to TEM observation. Next, these samples were observed using a field emission transmission electron microscope (Tecnai F20, FEI Inc., USA) at an acceleration voltage of 80 kV. Bright-field images of the AuNPs were obtained and processed using image processing software (Digital Micrograph, Gatan Inc., USA), after which the maximum diameter of 500 particles was measured manually. Furthermore, the precipitate extracted from the SPEED solution described above was prepared for TEM observation using the same method as for the AuNPs and observed using high-angle annular dark-field scanning transmission electron microscopy (HAADF-STEM).

2.4 Overview of the size separation principle and measurement conditions for AF4-ICP-MS

Figure 1(a) shows a schematic diagram of the Wyatt Eclipse AF4 system (Wyatt Technology Europe (Germany)), which was combined with the ICP-MS and FI equipment. This system was equipped with a pump for high-performance liquid chromatography, an integrated degassing system, and an autosampler (Agilent Technologies 1260 Infinity series, Agilent Technologies (USA)). After injecting nanoparticle samples into the AF4 separation channel, they were diffused and transported using the channel flow and separated based on their size as they move with the channel flow.

In AF4 analysis, the separation sequence consists of four steps: sample injection, focusing, relaxation, and elution.[16] First, after injecting the sample into the AF4 separation channel and waiting a short time, the sample is gradually collected to a single point by the flow from both horizontal sides of the AF4 separation channel. This step is called focusing (Fig. 1(b)). Subsequently, these particles diffuse upward, perpendicular to the AF4 separation channel. The distance of this diffusion depends on the particle size of the sample. That is, smaller particles can diffuse farther from the bottom of the AF4 separation channel. This step is called relaxation. Finally, in the elution step, changing the channel flow to unidirectional to exit allows each particle in the sample to be separated based on differences in flow velocity within the laminar flow (Fig. 1(c)). Consequently, smaller particles are detected with shorter retention times. At this point, samples diffuse based on their retention time; therefore, the diffusion coefficient of the sample must be considered for AF4 separation.[17]

In the AF4 analysis of this study, a 300 mg L^{-1} SDS solution or a 500 mg L^{-1} SC solution was used as the AF4 carrier solution. Moreover, a regenerated cellulose (RC) ultrafiltration membrane with a molecular weight cutoff of 30 kDa (RC 30 kDa, Microdyn–Nadir (Germany)) was used at the accumulation wall for the AF4 separation channel. Subsequently, the separation device with a 275 mm-long channel was employed, which was equipped with a 350 μm-thick or 490 μm-thick asymmetric diamond-shaped channel spacer. The AF4 separation channel was directly connected to the ICP-quadrupole MS equipment (Agilent 8800, Agilent Technologies, USA). The online elemental information on the nanoparticles separated by AF4 was obtained using ICP-MS.

The sample introduction system comprised a self-aspirating nebulizer (Conikal DC Nebulizer, Glass Expansion, Port Melbourne, Australia) and a Scott-type chamber equipped with a Peltier cooling apparatus.

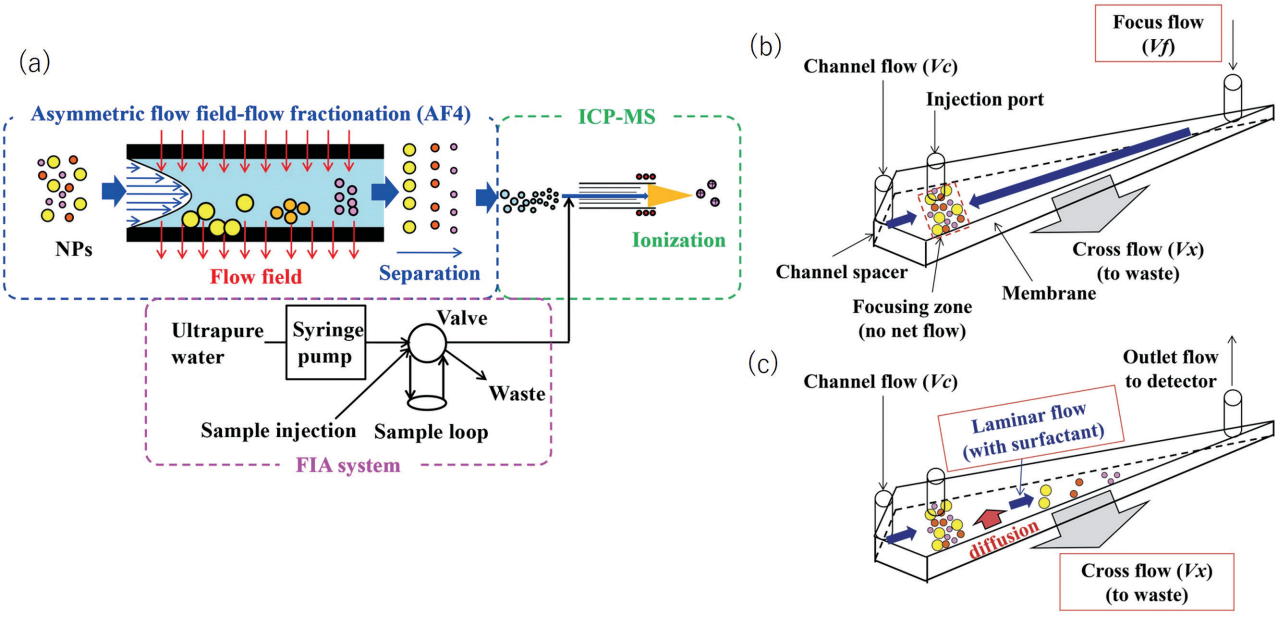

Fig. 1 (a) Schematic of AF4–ICP–MS and FI apparatus.[13] Flow profile observed during (b) the focusing step and (c) the elution step in the separation sequence of AF4 analysis.[12]

Table 2 summarizes the operating conditions in ICP-MS. Prior to the AF4 measurement, the membrane was conditioned with AF4 carrier solution of SDS or SC for at least 30 minutes. Each AuNP-dispersed solution was directly analyzed without dilution to maintain a good dispersion state in the sample vials. Precipitates dispersed in the SPEED solution were also analyzed without dilution. Additionally, injection of these samples into the AF4 separation channel was performed using an autosampler, and analysis was conducted for each. The AF4 separation conditions are summarized in **Table 3**.

2.5 Quantitative method using FI-AF4-ICP-MS

A new flow path (FI device) for flowing the standard solutions was installed independently from the AF4 equipment. **Figure 2** shows a schematic diagram of the FI device's flow path. Fig. 2(a) shows the flow path during sample insertion, and Fig. 2(b) shows the flow path during sample ejection. This flow path comprised a syringe pump, a six-way switching valve, and a sample loop. The syringe pump and six-way switching valve were connected to the nebulizer, and the sample loop was connected to the six-way switching valve. The sample loop volume was adjusted to 552 μL. Additionally, a washing flow path was connected to the six-way switching valve. The path could be changed using the six way switching valve. Gold standard solutions were diluted to concentrations of 0, 0.01, 0.025, 0.05, and 0.1 mg L^{-1}, respectively, and prepared to contain 5% (v/v) aqua regia as the matrix (denoted as Std 1–5). The multi-element standard solutions were diluted to concentrations of 0,

Table 2 ICP–MS operating conditions

Agilent8800 ICP-MS	
RF power (W)	1 550
Nebulizer gas flow (L min^{-1})	(a) 1.05 (b) 0.82
Make-up gas flow (L min^{-1})	0.23
Cooling gas (L min^{-1})	15
Auxiliary gas (L min^{-1})	0.9
Sampling depth (mm)	(a) 8 (b) 7
Element (m/z)	Nb (93), Au (197)
Duration time (s)	0.1
Spray chamber temperature (K)	275.15

(a) size distribution, (b) number concentration analysis

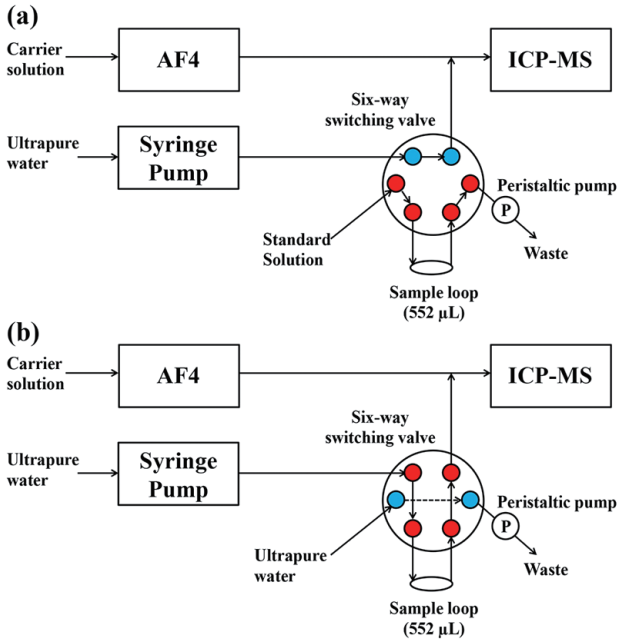

Fig. 2 Schematic of flow route of FI apparatus. (a) Sample load; (b) sample injection.[13)]

Table 3 AF4 separation condition

		For AuNPs	For AuNPs	For AgNPs	For NbC precipitates
Channel parameters	Membrane nature	Regenerated Cellulose (RC)			
	Membrane cut-off (kDa)	30	30	5	30
	Spacer (μm)	350	350	350	490
	Elution solvent	1.04 mmol L^{-1} SDS	1.04 mmol L^{-1} SDS	1.73 mmol L^{-1} SDS	0.035 mmol L^{-1} SDS
Fractionation time	Elution time (min)	1	35	1	1
	Focusing time (min)	1	0	1	1
	Focus + Injection time (min)	2	0	2	2
	Focusing time (min)	3	0	3	1
	Elution time (min)	35	0	35	45
Fractionation step, flow, and volume	Injection volume (μL)	1	1	100	20–100
	Injection flow (mL min^{-1})	0.2	0.2	0.2	0.2
	Channel flow (Vout, mL min^{-1})	1	1	1	1
	Cross flow (Vc, mL min^{-1})	Condition 1: 0.5 → 0 Condition 2: 1.5 → 0 Condition 3: 2.0 → 0 Condition 4: 3.0 → 0 Condition 5: 4.0 → 0 (linear gradient)	Condition 0: 0	3.0 → 0 (linear gradient)	2.0 → 0.1 (linear gradient)
	Focus flow (mL min^{-1})	3	0	3	3
Detector	UV absorbance (nm)	254	254	254	520

1.0, 3.0, 7.5, and 10 ng L^{-1}, respectively, and prepared to contain 1% (v/v) nitric acid as the matrix. These standard solutions were injected from the washing flow path to the sample loop under conditions that were unconnected to the nebulizer. After preparing the sample loop using the standard solutions,, the flow path was switched, and a constant volume of standard solutions was flowed to the nebulizer using a syringe pump. The standard solution was detected via time-resolved analysis, and the peak area of the signals detected via ICP-MS was integrated. The calibration curve was obtained from the correlation between the injected volume of the standard solution and the obtained peak area of the chromatogram.

3. Results and Discussion: Particle Size Distribution Analysis

3.1 TEM observations of each nanoparticle

First, AuNP-5.5, AgNPs, and NbC in the steel specimens were observed using TEM. **Figure 3** shows an example of bright-field TEM images of AuNP-5.5 and AgNPs and their measured particle size distributions. The AgNP size distribution was determined by measuring the diameter (Dmax), ignoring the thickness (Dw). AuNP-5.5 and AgNPs were dispersed not as aggregates but as single particles with a primary diameter. In contrast, as shown in **Fig. 4**, NbC was clearly aggregated in several observation fields. Regarding particle shape, most AuNP-5.5 and AgNP-50s were spherical, though some particles were not spherical. Furthermore, AgNP-50p and NbC were plate-like. The diameter and thickness of AgNP-50p were approximately 56 nm and 14 nm, respectively, while the diameter and thickness of NbC were several nm. The particle sizes of these nanoparticles were measured using the following AF4.

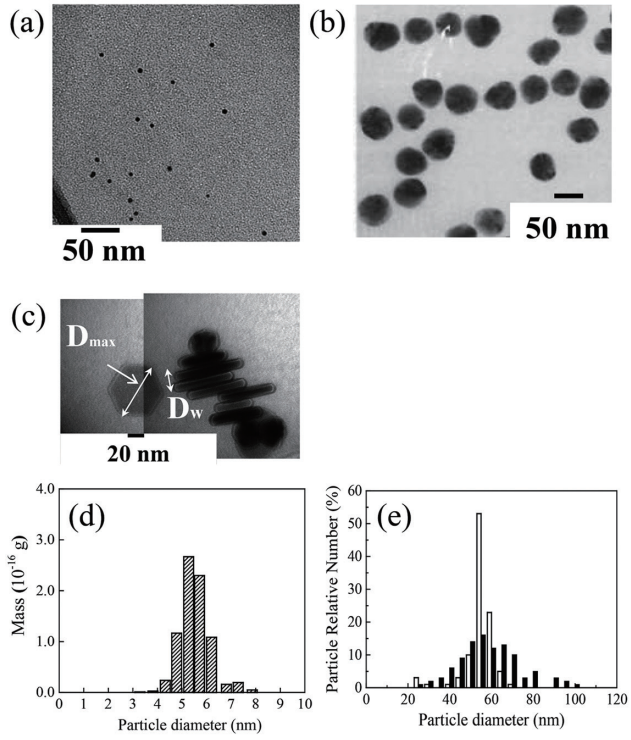

Fig. 3 TEM bright-field image of (a) AuNP-5.5, (b) AgNP-50s, and (c) AgNP-50p on a carbon-supporting grid. The size distribution of (d) AuNP-5.5 and (e) AgNPs determined by TEM.[12)]

3.2 Comparison of AF4 and TEM measurement results for AuNPs (average particle size and width of particle size distribution)

To confirm the performance of particle size measurement method for AF4, AuNP-5.5 (primary diameter 5.5±0.5 nm) was measured using both AF4 and TEM. First, AF4 measurements were performed under optimized conditions capable of adequately separating nanoparticles of several nanometers. The particle size distribution of AuNP-5.5 was estimated using the calibration curve obtained based on the correlation between particle size and retention time for other AuNPs. The AF4 measurement results were fitted via a Gaussian distribution, and the average particle size of AuNP-5.5 and the full width at half maxima (FWHM) of the particle size distribution were calculated. Next, for the TEM observation of AuNP-5.5, the measurement was repeated twice to confirm the uncertainty of particle size measurement using TEM.

Tables 4 and **5** summarize the average particle size and FWHM of the particle size distribution for AuNP-5.5, respectively. First, comparing the average particle sizes obtained by AF4 and TEM, as shown in Table 4, the two values agreed well as expected. This is likely because AF4 measurement was conducted using the size calibration curve with TEM results.

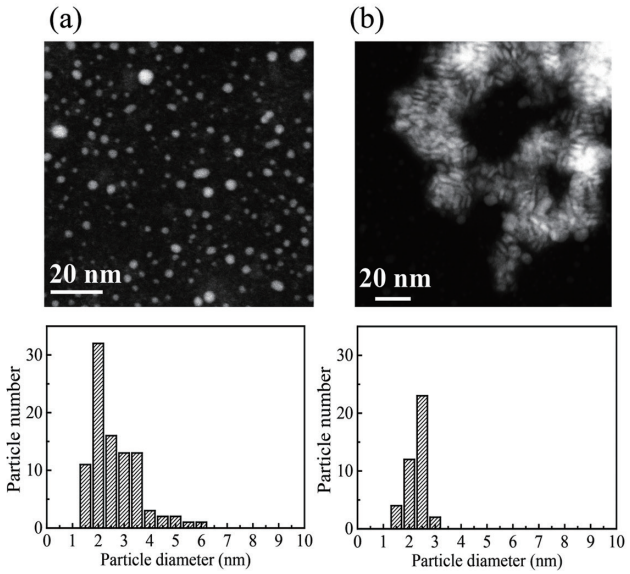

Fig. 4 HAADF-STEM image of electrolytically extracted NbC from the steel sheet, NCA5-3, at two FOVs and size distributions at each FOV[12)]: (a) FOV No.1 and (b) FOV No.2.

Table 4 Average diameter of each specimen measured by TEM and AF4

Sample	Average diameter (nm)		
	TEM	AF4 (raw data)	AF4 (corrected)
AuNP-5.5	5.5 ± 0.5	5.6 ± 1.0	5.6 ± 0.5
AgNP-50s	52.1 ± 7.1	54.1 ± 11.1	–
AgNP-50p	56.2 ± 14.6	59.6 ± 23.0	–
NbC precipitates in NCA5-1	–	2.1 ± 0.5	2.1 ± 0.2
NbC precipitates in NCA5-3	2.4 ± 1.0 (FOV-1) 2.1 ± 0.4 (FOV-2)	2.0 ± 0.4	2.0 ± 0.2

Table 5 Results of particle size distribution analysis and broadening factors in AF4 analysis

Ti	Average diameter (nm) (TEM)	Shape	Component of materials	Density/g·cm^{-3}	Broadening factor	FWHM (AF4)	FWHM (TEM)
AuNP-2	2.1 ± 0.3	Sphere-like	Gold	19.32	2.21	1.66	0.75
AuNP-5	5.0 ± 0.6	Sphere-like	Gold	19.32	2.05	2.56	1.25
AuNP-5.5	5.5 ± 0.5	Sphere-like	Gold	19.32	1.94	2.4	1.24
AuNP-7	7.5 ± 0.8	Sphere-like	Gold	19.32	2.29	3.09	1.35
AuNP-10	9.8 ± 0.8	Sphere-like	Gold	19.32	1.94	3.47	1.79
AgNP-50s	52.1 ± 7.1	Sphere-like	Silver	10.49	3.01	26.09	8.66
AgNP-50p	56.2 ± 14.6	Plate-like	Silver	10.49	1.64	54.05	32.9

Next, comparing the FWHM of the particle size distribution shown in Table 5, the AF4 measurement results were not consistent with the TEM results. The FWHM of the AF4 results were approximately twice the values obtained by TEM. This difference is thought to be due to the following two reasons. First, the characterization of the particles used in this study employed multiple measurement methods based on different principles. AF4 measures particle mobility, while TEM measures electron beam diffraction. Consequently, AF4 results reflect the outer shape and size of the particles, whereas TEM results indicate the contrast of electron diffraction derived from elemental components and crystalline nature. Therefore, differences in assumptions regarding particle shape likely reflected in these results.

Second, considerable attention should be paid to the measurement method in AF4 analysis, because the FWHM of the particle size distribution measured by AF4 was larger than that obtained by TEM due to the diffusion of the particles in the AF4 separation channel. Because AF4 measurements are conducted under the condition that particles were flowing, it was unavoidable that any particle would diffuse in the AF4 separation channel. This phenomenon led to the broadening of the particle size distribution and a lack of size resolution. Consequently, the particle size distribution measurement method using AF4 requires improvement.

3.3 Correction of particle size distribution width in AF4 analysis

As discussed in the previous section, the FWHM of the particle size distribution in AF4 measurements is highly dependent on the measurement principle. Therefore, we investigated methods to correct AF4 measurement results based on other analytical techniques. The proposed correction method for the FWHM in AF4 particle size distribution measurements is as follows. For the particle size distribution of AuNP-5.5, the ratio of the AF4 FWHM to the TEM FWHM, as shown in Table 5, was 1.94. This value was defined as the broadening factor for AF4 analysis. Furthermore, the broadening factors calculated for other nanoparticles using the same method are shown in Table 5. Note that the two types of AgNPs had particle diameters approximately 10 times larger than the above AuNPs, necessitating measurement under different AF4 operating conditions. Additionally, prior to the AF4 measurement of the AgNPs, a calibration curve for particle size measurement was obtained using several AuNPs and PSL particles (**Fig. 5**). **Figure 6** shows the particle size distributions of the two types of AgNPs measured by AF4 and TEM. The results revealed that particle diffusion within the AF4 separation channel can affect the AF4 chromatogram, regardless of particle size. The findings regarding the broadening factor are summarized below.

(i) The broadening factor calculated from the above AuNPs mea-

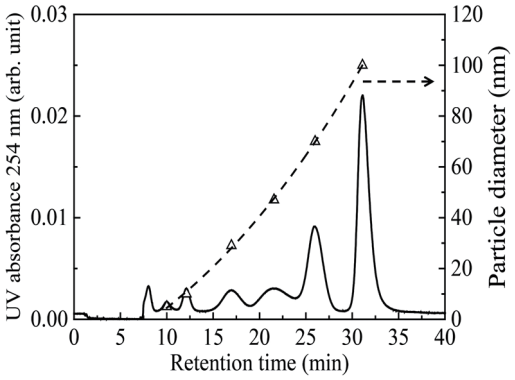

Fig. 5 Separation results of AuNPs and PSL mixtures by AF4.[12] Bottom and right axes show the size calibration curve.

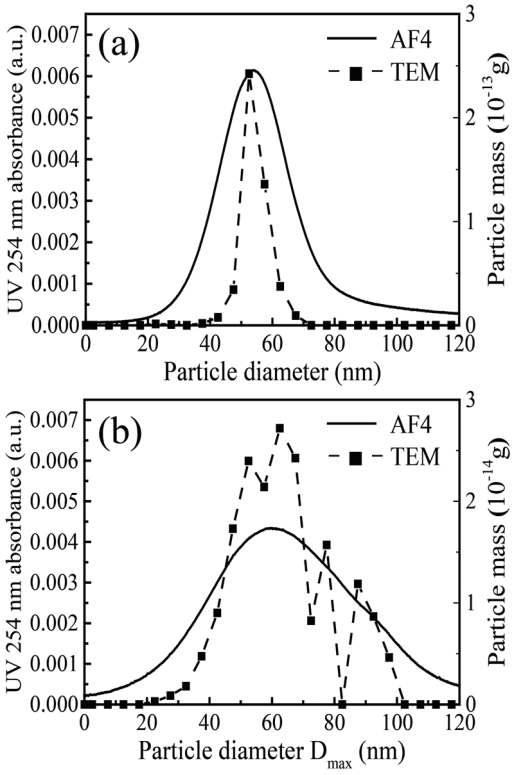

Fig. 6 Size distributions of AgNPs measured using TEM and AF4. (a) AgNP-50s and (b) AgNP-50p.[12]

surement results largely depends on particle shape and type. The broadening factor determined for sphere-like particles ranged from 1.94 to 2.29.

(ii) Since direct comparisons between different particle types are difficult, the influence of particle shape on two types of AgNPs was examined as follows. The broadening factor for plate-like particles appeared smaller than that for sphere-like particles. This is attributed to the fact that the flow within the AF4 separation channel becomes dominant over the Brownian diffusion of the plate-like particles themselves. Consequently, the Brownian motion of plate-like particles is thought to be suppressed horizontally relative to the flow within the AF4 separation channel.

3.4 Application of the AF4 particle size distribution measurement method with broadening factor to NbC in steels

To investigate the applicability of FWHM correction method in AF4 analysis, NbC precipitates extracted from steel specimens were measured using AF4. The results showed that FWHM correction method is effective for more accurately measuring the particle size of nanometer-sized precipitates in steels.

First, NbC was measured under the same AF4 measurement conditions as AuNPs. **Figure 7** shows the particle size distribution of NbC measured by AF4 and corrected by applying the broadening factor. Heat treatment was applied to these samples to increase the NbC particle size, and it was expected that the particle size of NCA5-3, which underwent longer heat treatment, would be larger. However, TEM observation of these NbC particles revealed that they were ununiformly dispersed within the steel specimens, and their particle sizes did not change significantly. Although the NbC particle size distribution obtained by TEM sometimes did not match between fields of view, as shown in Fig. 4, the results were close to those obtained by AF4, which provides average particle size distribution information. It became clear that the NbC particle size did not change with increasing heat treatment holding time, while the number concentration increased (approximately 1.5 times in peak area).

4. Results and Discussion: Quantification of Number Concentration

4.1 Calibration curve creation in FI-AF4-ICP-MS analysis

Gold standard solutions and AuNP-2 were analyzed using only the AF4-ICP-MS, and the peak areas of each chromatogram were compared. The peak area of AuNP-2 was approximately 3.3 times larger than that of the gold standard solution, despite the gold injection volume into the AF4 separation channel being about half that of the gold standard solution. The reason for the significant reduction in the amount of gold introduced into the ICP-MS for the gold standard solution is thought to be that a large amount of gold ions passed through the permeable membrane inside the AF4 separation channel and was removed as waste solution. From the above results, it became clear that the injection of the gold standard solution into the AF4 separation channel is not suitable for obtaining an accurate calibration curve.

Therefore, to achieve accurate quantification of analytical results obtained by the AF4-ICP-MS method, the application of the FI method was investigated. First, the method for preparing a calibration curve using gold standard solutions was examined. To achieve matrix matching in ICP-MS analysis, the AF4 carrier solution was prepared at twice the concentration used in AF4 analysis. Immediately before the nebulizer, the AF4 carrier solution was rapidly mixed with an gold standard solution containing 5% (v/v) aqua regia or 1% (v/v) nitric acid in an equal volume ratio. **Figure 8** shows the FI chromatograms of the gold standard solutions (Std 1–5) when ultrapure water was used as the AF4 carrier solution. The peaks in each chromatogram of Std 1–5 were integrated, and a calibration curve was constructed using these peak areas. **Figure 9** shows the calibration curves obtained when applying the FI method to the gold standard solutions prepared using each AF4 carrier solution. When SDS solution was used as the AF4 carrier solution, the calibration

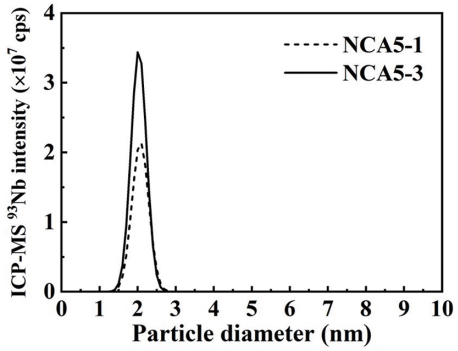

Fig. 7 Results of AF4-ICP-MS measurement for NbC in steels NCA5-1 and NCA5-3[12)]

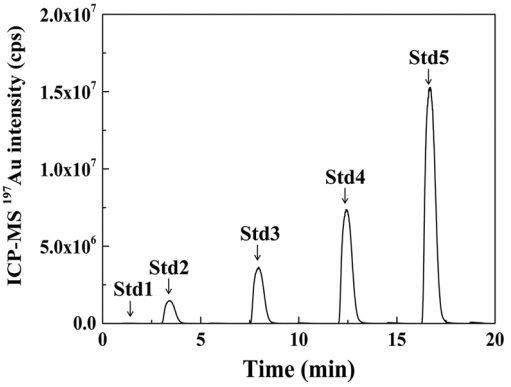

Fig. 8 FI chromatogram of Au standard solution (Std 1–5)[13)]

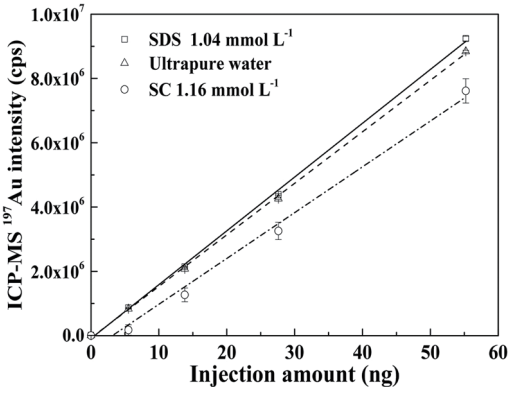

Fig. 9 Comparison of FI calibration curves of the Au standard solution among ultrapure water (△), SDS solution (□), and SC (○) solution[13)]

curve exhibited good linearity, yielding results nearly equivalent to those obtained with ultrapure water as the AF4 carrier solution. In contrast, when SC solution was used as the AF4 carrier solution, good linearity of the calibration curve could not be achieved, and the variation at each point was large. This was caused by the differences in the acid dissociation constants of each surfactant in AF4 carrier solution. The acid dissociation constants for SDS and SC are 1.84 and 4.98, respectively. When mixing a 5% (v/v) aqua regia-containing gold standard solution with each surfactant solution, the solution pH is expected to be lower than the acid dissociation constant of SC. Even when SDS solution and 5% (v/v) aqua regia were mixed at the same volume ratio, the solution remained transparent. However, salt precipitation was observed in the solution when SC solution and 5% (v/v) aqua regia were mixed at the same volume ratio. This suggests that salt precipitation from SC caused blockage of the nebulizer or PFA tube, preventing stable ICP-MS signals. Consequently, significant signal intensity variation occurred in the calibration curve using the FI method. Therefore, it became clear that SC solution is unsuitable for FI-AF4-ICP-MS analysis due to the inability to obtain stable signal intensity. Therefore, it is considered necessary to appropriately select surfactants for this analysis, taking into account their acid dissociation constants.

4.2 Quantification of AuNPs by FI-AF4-ICP-MS analysis

To investigate the accuracy and precision of the FI method, AF4-ICP-MS analysis of AuNPs was performed. For the AuNPs detected by AF4-ICP-MS analysis, each was quantified using the calibration curve obtained by applying the FI method. The accuracy and precision in this analysis were evaluated using the recovery rate shown in Equation (1). Furthermore, considering sampling uncertainty, an equal amount of AuNPs was analyzed by AF4-ICP-MS under conditions where only channel flow was flowed through the AF4 separation channel. The injected amount was determined by quantifying the detected amount using the calibration curve obtained from the FI method.

$$\text{Recovery (\%)} = \frac{\text{The amounts quantified by FI analysis (g)}}{\text{The injected amounts of samples (g)}} \times 100 \quad (1)$$

This study investigated the effect of sample retention time (t_R) on recovery rates obtained by AF4 analysis. AF4 separation conditions can be adjusted by modifying the channel flow rate, cross-flow rate, AF4 separation channel volume, temperature, and solvent viscosity, as shown in Equation (2)[10, 11]. In particular, the channel flow rate and cross-flow rate were the easiest parameters to adjust, to change AF4 separation conditions.

$$t_R = \frac{w^2 R_h \pi \eta}{kT} \ln\left(1 + \frac{V_c}{V_0}\right) \quad (2)$$

where V_0 is the channel flow rate, V_c is the cross-flow rate, w is the spacer thickness, η is the solvent viscosity, k is the Boltzmann constant, T is the absolute temperature, and R_h is the hydrodynamic diameter.

In this study, only the cross-flow rate was varied to change the AF4 separation conditions, thereby altering the retention time of the sample. **Figure 10**(a) shows the chromatograms of the AF4-ICP-MS analysis of AuNP-50 under each AF4 separation condition (Condition 1 to 5, 0) listed in Table 3. Increasing the cross-flow rate tended to prolong the retention time of AuNP-50. Furthermore, the recovery rate of AuNP-50 is shown in Fig. 10(c). It was found that the recovery rate of AuNP-50 decreased as the retention time increased, with the effect becoming significant when the retention time exceeded 25 minutes. This result is thought to be caused by the aggregation of AuNP-50 and its adsorption onto the permeable membrane inside the AF4 separation channel. As shown in Fig. 10(b), peaks originating from AuNP-50 aggregates were observed under AF4 separation conditions 2 to 5. Although the recovery rate was calculated without considering these aggregate-derived peaks in this study, even if these peaks were accounted for, the recovery rate did not reach 100%. This indicates that not only did AuNP-50 aggregate, but also that a portion of the AuNP-50 adsorbed onto the permeable membrane inside the AF4 separation channel and was not detected by ICP-MS. Therefore, the sample retention time in AF4 analysis must be adjusted to be within 20 minutes.

Furthermore, five types of AuNPs were analyzed via AF4-ICP-

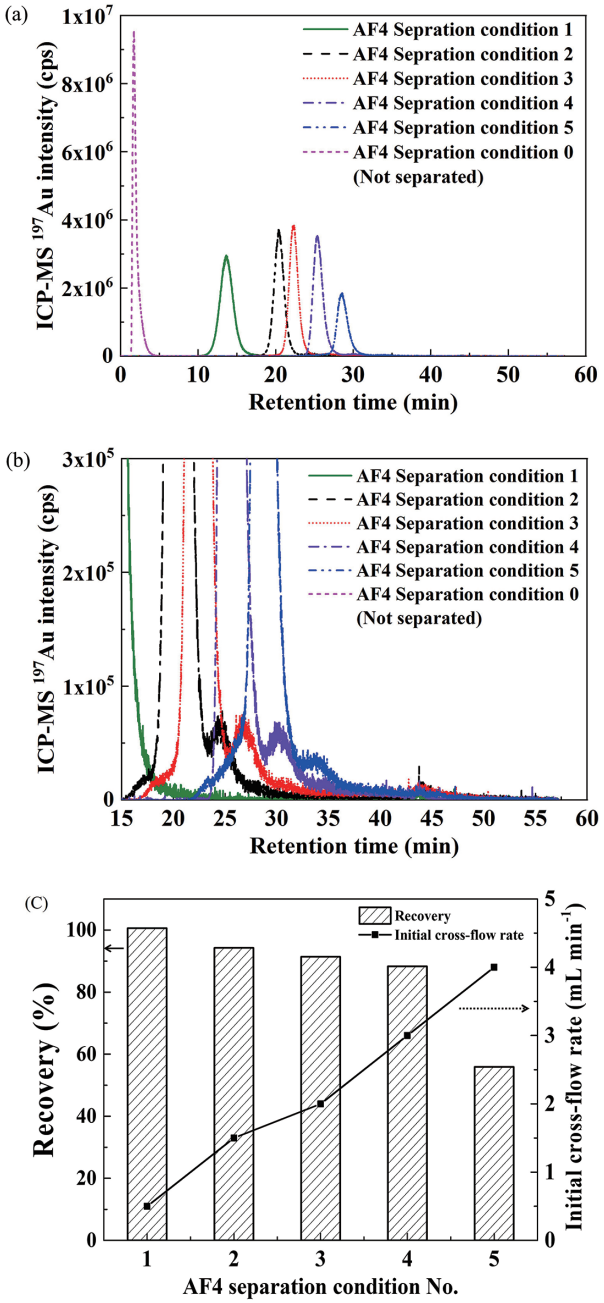

Fig. 10 (a) AF4–ICP–MS chromatogram, (b) enlarged part of (a) and (c) recovery of AuNP-50 under each AF4 separation condition[13]

MS thrice under appropriate AF4 separation conditions and quantified using FI method. The recovery rates for each AuNP are shown in **Fig. 11**. Good analytical performance was achieved by the developed FI method. Recovery rates exceeded 93% for all, with coefficient of variation within 5%. While no effect of particle size on recovery was observed, variations in sample collection and the dispersion state of the sample may have contributed to slight recovery rate reductions.

4.3 Quantification of NbC in steel samples by FI-AF4-ICP-MS analysis

Figure 12 shows the number concentration of NbC as determined by the FI-AF4-ICP-MS method. Using the average diameter (approximately 2 nm)[9] measured by the AF4 method and the density of NbC, the mass of Nb quantified by FI-AF4-ICP-MS analysis was converted to the number concentration of NbC. The steel specimens used in this test were aged at 873 K for either 1 hour (NCA5-1) or 10 hours (NCA5-3). It was found that increasing the aging time increased the number concentration of NbC by approximately 6-fold. Furthermore, TEM observations confirmed that these NbC particles were ununiformly dispersed within the steel, making it impossible to accurately evaluate the number concentration via TEM observation. In contrast, FI-AF4-ICP-MS analysis can analyze more precipitates in steel than TEM or atom probe tomography (APT), making it advantageous from the perspective of sample representativeness. Therefore, FI-AF4-ICP-MS analysis is considered an effective analytical method for quantitatively analyzing the size and number concentration of precipitates in steel.

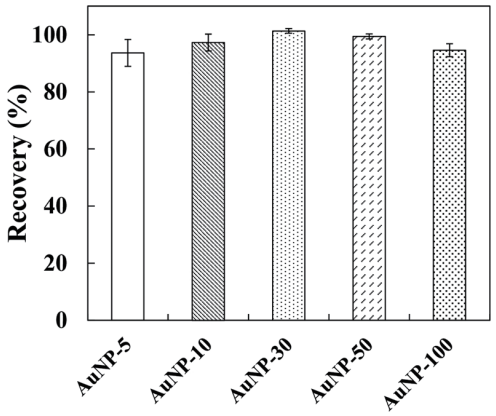

Fig. 11 Recovery of AuNPs in AF4–ICP–MS analysis[13]

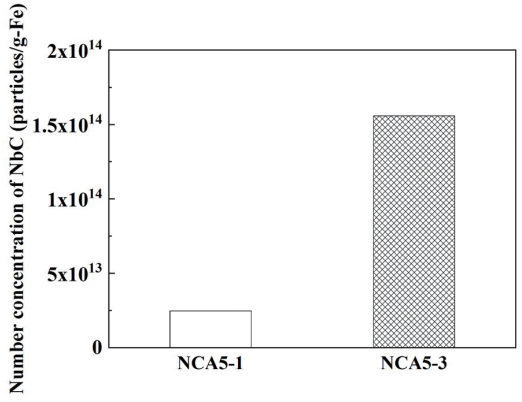

Fig. 12 Quantification of number concentration of NbC precipitates in NCA5-1 and NCA5-3 steels[13]

Based on the above findings, the application of FI method to AF4-ICP-MS analysis enables quantitative analysis of various nanoprecipitates in steel samples. However, since this analytical method involves extracting precipitates from steel, the spatial information within the steel specimen is lost. Therefore, AF4-ICP-MS analysis should be used complementarily with local observation techniques such as TEM or APT. Such multifaceted evaluation is considered essential for interpreting various phenomena in the steel manufacturing process.

5. Conclusion

This study investigated methods for measuring particle size distributions using AF4 coupled with TEM for various nanoparticles. Furthermore, quantitative methods for AF4-ICP-MS analysis using the FI method were examined using AuNPs, and NbC in steel. The findings obtained in this study are summarized below.

(1) The average particle size measured by AF4 was nearly consistent with that measured by TEM.
(2) In AF4 measurements, peak broadening occurs due to particle diffusion within the AF4 separation channel.
(3) It was confirmed that the FWHM of the particle size distribution in AF4 analysis can be corrected using the broadening factor, defined as the AF4/TEM FWHM ratio.
(4) The broadening factor for sphere-like particles was determined to be approximately 2.0. However, the broadening factor for plate-like particles (approximately 1.6) was apparently smaller than that for sphere-like particles due to suppression of Brownian motion.
(5) To achieve proper matrix matching, the standard solutions required for obtaining calibration curves must be mixed with the AF4 carrier solution. The surfactant used in this AF4 carrier solution must be selected considering the acid dissociation constant of the surfactant.
(6) To prevent sample aggregation within the AF4 separation channel and sample adsorption onto the permeable membrane inside the AF4 separation channel, the separation conditions must be adjusted so that the sample retention time in AF4 analysis is kept within 20 minutes.
(7) FI-AF4-ICP-MS analysis quantitatively demonstrated that increasing the aging treatment time of steel specimens from 1 h to 10 h results in approximately a six-fold increase in the number concentration of fine NbC particles.

These results demonstrate that applying a broadening factor makes AF4 analysis effective for evaluating particle sizes of various nanoparticles, indicating the applicability of FWHM correction in AF4 analysis. Furthermore, since FI method is effective for quantitative evaluation of various nanoparticles using AF4-ICP-MS analysis, this analytical method is considered a useful technique for determining the size distribution and number concentration of various precipitates in steel.

References

1) Kamikawa, N. et al.: ISIJ Int. 54 (1), 212 (2014)
2) Kataoka, T. et al.: ISIJ Int. 56 (11), 2062 (2016)
3) Ohta, H. et al.: ISIJ Int. 48 (3), 294 (2008)
4) Kinoshiro, S. et al.: Tetsu-to-Hagané. 99 (5), 362 (2013)
5) Wei, G.-T. et al.: Anal. Chem. 71 (11), 2085 (1999)
6) Krueger, K. M. et al.: Anal. Chem. 77 (11), 3511 (2005)
7) Gray, E. P. et al.: J. Anal. At. Spectrom. 27 (9), 1532 (2012)

8) Liu, F.-K. et al.: J. Chromatogr. A. 1062 (1), 139 (2005)
9) Xu, X. et al.: J. Chromatogr. A. 1167 (1), 35 (2007)
10) Giddings, J.C. et al.: Science. 193 (4259), 1244 (1976)
11) Giddings, J.C.: Science. 260 (5113), 1456 (1993)
12) Itabashi, D. et al.: ISIJ Int. 60 (5), 979 (2020)
13) Itabashi, D. et al.: ISIJ Int. 62 (5), 860 (2022)
14) Takimoto, K. et al.: J. Jpn. Inst. Met. 40 (8), 834 (1976)
15) Kurosawa, F. et al.: J. Jpn. Inst. Met. 43 (11), 1068 (1979)
16) Kato, H.: AIST Bulletin of Metrology. 6 (4), 185 (2007)
17) Schimpf, M.E. et al.: Field-Flow Fractionation Handbook. New York, Wiley-Interscience, 2000

Daisuke ITABASHI
Ph.D., Senior Researcher
Materials Characterization Research Lab.
Advanced Technology Research Laboratories
20-1 Shintomi, Futtsu City, Chiba Pref. 293-8511

Shunsuke TANIGUCHI
Senior Researcher
Materials Characterization Research Lab.
Advanced Technology Research Laboratories

Kazumi MIZUKAMI
Ph.D., Senior Specialist
Futtsu Sales Office
East Japan Area Sales Department
Sales Division, Head Office
Nippon Steel Technology Co., Ltd.